Experimental test of nonlocal causality

QUANTUM PHYSICS

Experimental test of nonlocal causality

Martin Ringbauer,[1,2]* Christina Giarmatzi,[1,2] Rafael Chaves,[3,4,5] Fabio Costa,[1] Andrew G. White,[1,2] Alessandro Fedrizzi[1,2,6]

10.1126/sciadv.1600162

Explaining observations in terms of causes and effects is central to empirical science. However, correlations between entangled quantum particles seem to defy such an explanation. This implies that some of the fundamental assumptions of causal explanations have to give way. We consider a relaxation of one of these assumptions, Bell's local causality, by allowing outcome dependence: a direct causal influence between the outcomes of measurements of remote parties. We use interventional data from a photonic experiment to bound the strength of this causal influence in a two-party Bell scenario, and observational data from a Bell-type inequality test for the considered models. Our results demonstrate the incompatibility of quantum mechanics with a broad class of nonlocal causal models, which includes Bell-local models as a special case. Recovering a classical causal picture of quantum correlations thus requires an even more radical modification of our classical notion of cause and effect.

INTRODUCTION

Four decades after Freedman and Clauser (*1*) performed the first Bell's inequality test (*2*), a series of loophole-free experiments (*3*–*5*) have now conclusively shown that the predictions of quantum mechanics are at odds with local realism. Scientific realism posits that physical systems have real, objective properties—independent of whether we observe them or not—that determine the outcomes of measurements performed on the system. The idea of locality—or more precisely local causality—is that causal influences cannot propagate faster than the speed of light. On the basis of local causality, and the assumption that measurement settings can be chosen freely, Bell derived an inequality that must be respected by any set of correlations that can be explained in terms of, possibly hidden, common causes (see Fig. 1A) but is violated by observed quantum correlations. Consequently, a new area of research has emerged, exploring to what extent the various underlying assumptions have to be relaxed to recover a causal explanation of quantum correlations (*6*–*14*).

A natural framework for this research program, and the study of Bell's theorem, is the theory of causal modeling (*11*, *12*), which aims to explain correlations in terms of cause-and-effect relations between events (*15*, *16*). Discovering these relations from empirical data is difficult in general (*17*–*20*); however, within classical physics, such an explanation should always exist because the properties of a classical system, even if not measured, can always be assumed to have well-defined values. Causal reasoning is at the heart of empirical science and builds upon the most fundamental understanding of causality—that if a variable acts as the cause for another one, actively intervening on the first should cause changes in the second. More recently, causal modeling has attracted considerable interest in foundational physics, particularly for the study of stronger-than-classical correlations (*12*, *21*–*28*), dynamical causal order (*29*), and indefinite causal structures (*29*, *30*), and their role as computational resource (*31*–*34*).

Phrasing Bell's theorem in the language of causal models provides a clear picture of the underlying assumptions and allows for a unified and quantitative approach to relaxations of these assumptions (*11*, *12*). For example, quantum correlations can be explained by causal models when relaxing Bell's local causality assumption, which is commonly referred to as quantum nonlocality. Here, we test nonlocal causal models, which relax local causality by abandoning causal outcome independence and allowing for a causal influence from one measurement outcome to the other (see Fig. 1B). First, we consider the simplest case that reveals such correlations, the Clauser-Horne-Shimony-Holt (CHSH) scenario (*35*), where two parties, Alice and Bob, can each measure one of two dichotomic observables. Using controlled interventions, we find the potential causal influence insufficiently strong to explain the observed CHSH violation. In the second experiment, we go beyond the CHSH scenario and violate a Bell-type inequality, which involves three measurement settings for each party and is satisfied even for arbitrarily strong causal influences from one outcome to the other (*11*). In contrast to the interventional method, which requires detailed knowledge of the physical system under consideration, the latter method is device-independent. Our results highlight the incompatibility of quantum correlations not only with the well-known Bell-local causal models but also with nonlocal causal models, where one measurement outcome may have a direct causal influence on the other.

RESULTS

Theoretical background

A causal structure underlying n jointly distributed discrete random variables $(X_1, \ldots, X_n)$ is represented by a directed acyclic graph, where the nodes (circles in Fig. 1) represent variables and the directed edges (arrows in Fig. 1) represent causal relations (*15*). Bell's theorem, where two observers, Alice and Bob, perform local measurements on one

[1]Centre for Engineered Quantum Systems, School of Mathematics and Physics, University of Queensland, Brisbane, Queensland 4072, Australia. [2]Centre for Quantum Computation and Communication Technology, School of Mathematics and Physics, University of Queensland, Brisbane, Queensland 4072, Australia. [3]Institute of Physics and Freiburg Center for Data Analysis and Modeling, University of Freiburg, 79104 Freiburg, Germany. [4]Institute for Theoretical Physics, University of Cologne, 50937 Cologne, Germany. [5]International Institute of Physics, Universidade Federal do Rio Grande do Norte, 59070-405 Natal-RN, Brazil. [6]School of Engineering and Physical Sciences, Scottish Universities Physics Alliance, Heriot-Watt University, Edinburgh EH14 4AS, UK.
*Corresponding author. Email: m.ringbauer@uq.edu.au

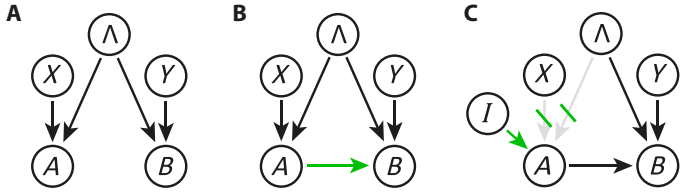

Fig. 1. Causal structures for a Bell scenario. (**A**) Bell's original local hidden-variable models, where X (Y) is Alice's (Bob's) measurement setting, and A (B) is the corresponding measurement outcome. Λ denotes the local hidden variable. (**B**) A relaxation of local causality, where A may have direct causal influence on B. The Bell-local models in (A) are the limiting case where the green arrow from A to B vanishes. An explicit example of such a model is given in the Supplementary Materials. (**C**) An intervention (I) on A forces the variable to take a specific value and breaks all incoming arrows.

half of a shared quantum state, can be conveniently formulated in this language. Figure 1A shows the corresponding causal graph, based on Bell's assumptions of measurement independence and local causality. Measurement independence states that the measurement choices of Alice and Bob, X and Y, respectively, are independent of how the system has been prepared, that is, there is no causal link from the hidden variable Λ to X or Y and thus $p(x,y,\lambda) = p(x,y)p(\lambda)$. Local causality implies that the probability of Alice's (Bob's) outcome A (B) is fully specified by Λ and by the measurement choice X (Y), that is, $p(a|x,y,b,\lambda) = p(a|x,\lambda)$ and $p(b|x,y,a,\lambda) = p(b|y,\lambda)$. Here and in the following, we adopt the usual convention that uppercase letters denote random variables, whereas their values are denoted in lowercase. Interpreted in the causal modeling framework, local causality is the combination of what we call causal parameter independence—there is no direct causal influence from the measurement setting Y (X) to the other party's outcome A (B)—and causal outcome independence, stating that there is no direct causal influence from one outcome to the other. Note that these definitions are motivated by the causal structure and differ from the statistical notion of outcome independence and parameter independence (*36*), which cannot be given a causal interpretation (see Materials and Methods for details).

The causal models compatible with these assumptions are the well-known Bell-local hidden-variable models: $p(a,b|x,y) = \Sigma_\lambda p(a|x,\lambda)p(b|y,\lambda)p(\lambda)$. The constraints on the observable probabilities $p(a,b|x,y)$ dictated by such a causal model are known as Bell inequalities. In the simplest possible Bell scenario, where each of the parties measures one of two observables ($x,y = 0,1$) obtaining one of two possible outcomes ($a,b = 0,1$), any correlations compatible with Bell-local causal models must respect the CHSH inequality (*35*)

$$S_2 = \langle A_0B_0\rangle + \langle A_0B_1\rangle + \langle A_1B_0\rangle - \langle A_1B_1\rangle \leq 2 \qquad (1)$$

where $\langle A_xB_y\rangle = \sum_{a,b\,=\,0,1}(-1)^{a\,+\,b}p(a,\,b|x,\,y)$ is the joint expectation value of A_x and B_y. The first loophole-free Bell experiments (*3*–*5*) now conclusively show that quantum mechanics allows for correlations that violate this inequality, therefore witnessing its incompatibility with causal models that satisfy local causality and measurement independence.

To retain a classical causal explanation for the correlations observed in the Bell scenario, some of these causal assumptions have to be relaxed (*7*–*14*, *36*). We focus on the class of models that satisfy causal parameter independence, but do not assume causal outcome independence, such that Alice's measurement outcomes may have a direct causal influence on Bob's outcomes (see Fig. 1B). The same arguments hold for the case where Bob's outcome influences Alice's outcome (with the $A\rightarrow B$ arrow reversed in Fig. 1B), or any linear combination of these cases, as discussed in detail in the Supplementary Materials. Because the causal model is formulated without any reference to a space-time structure, this influence may be sub- or superluminal, instantaneous, or even to the past, as long as it does not create any causal loop. In particular, it is consistent with a recent no-go theorem, which states that quantum correlations cannot be explained by any finite-speed influence (*37*). The probability distributions compatible with this causal structure can be decomposed as

$$p(a,b|x,y) = \sum_\lambda p(a|x,\lambda)p(b|y,a,\lambda)p(\lambda) \qquad (2)$$

Interventional method

The first experimental method we use to test this model relies on interventions, a core tool in causal discovery that allows for the identification and quantification of causal influences (*11*, *15*, *38*, *39*). Formally, an intervention is the act of locally forcing a variable X_i to take on some value x'_i, denoted $do(x'_i)$. This removes all incoming arrows on X_i while keeping the causal dependencies between all other variables unperturbed (see A in Fig. 1C). In practice, performing such arrow-breaking interventions always requires some background knowledge of the system under consideration because the possible persistence of "confounding" common causes cannot be excluded from statistics alone. In our case, we shall assume that, for the purpose of the intervention, the local degrees of freedom behave according to quantum mechanics. Such assumptions are common in quantum steering scenarios and semi–device-independent quantum cryptography, where it is assumed that the devices of at least one of the laboratories can be trusted and work according to quantum mechanics.

In the CHSH scenario, passive observations alone are not enough to determine whether correlations between A and B are due to direct causation or a common cause Λ. However, an intervention on variable A would break the link between A and the (hypothetical) variable Λ. Thus, all remaining correlations between A and B must stem from direct causation. The maximal shift in the probability distribution of B upon intervention on A allows quantifying the strength of this causal link (*11*). To achieve this, we use the so-called average causal effect (ACE) (*15*, *38*)

$$\mathrm{ACE}_{A\rightarrow B} = \sup_{b,y,a,a'}\left|p\left(b|do(a),y\right) - p\left(b|do(a'),y\right)\right| \qquad (3)$$

which is a variant of the measure $\boldsymbol{C}_{A\rightarrow B}$ used in the work of Chaves *et al.* (*11*). In contrast to the latter, $\mathrm{ACE}_{A\rightarrow B}$ does not require knowledge of the hidden variable and is thus experimentally accessible. As we prove in detail in the Supplementary Materials, the average causal effect satisfies the same relation as $\boldsymbol{C}_{A\rightarrow B}$ in the work of Chaves *et al.* (*11*), namely

$$\mathrm{ACE}_{A\rightarrow B} \geq \max[0, (S_2 - 2)/2] \qquad (4)$$

where the maximum is taken over all eight symmetries of the CHSH quantity under relabeling of inputs, outputs, and parties (*35*). That is,

the average causal effect required for a causal explanation of a set of quantum correlations is directly proportional to the CHSH violation achieved by the correlations in question.

We experimentally implemented an intervention on a CHSH-Bell test using pairs of polarization-entangled photons, generated in the state $\cos\gamma|HV\rangle + \sin\gamma|VH\rangle$ (see Fig. 1A). Here, H and V correspond to horizontal and vertical polarizations, respectively, and γ is the polarization angle of the pump beam, which continuously controls the degree of entanglement, as measured by the concurrence $\boldsymbol{C} = |\sin(2\gamma)$ (*40*).

Alice and Bob test the CHSH inequality with two settings and two outcomes each. The measurements are chosen in the equatorial (linear polarization) plane of the Bloch sphere (see Fig. 2B). To test the (directional) link $A \rightarrow B$, Bob was located in the causal future of Alice using a 2-m fiber delay before Bob's measurement device. Recall that an intervention on Alice's outcome A needs to break all relevant incoming causal arrows and deterministically set the value of the variable A. Relying on the quantum description of the local degrees of freedom, these requirements are met by first projecting Alice's photon onto circular polarization states $|R/L\rangle = (|H\rangle \pm i|V\rangle)/\sqrt{2}$—which, within experimental precision, erases all relevant information for the CHSH test performed in the linear polarization plane—and then re-preparing it in eigenstates of Alice's measurement PBS $|H/V\rangle$—which forces one of the two outcomes $A = \pm 1$. This corresponds to operations of the form $|H/V\rangle\langle R/L|$, which are experimentally implemented using a quarter-wave plate at ±45°, followed by a polarizer directly before Alice's measurement PBS. The measurement bases for Alice and Bob, as well as the setting of the intervention polarizer and quarter-wave plate, were chosen randomly using quantum random numbers from the Australian National University's online quantum random number generator based on the work of Symul *et al.* (*41*).

Single-photon clicks in the avalanche photodiodes for each outcome are registered with an AIT-TTM8000 time-tagging module with a temporal resolution of 82 ps. Outcome probabilities, used to estimate

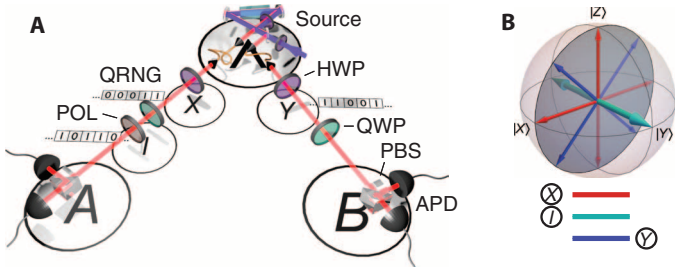

Fig. 2. The experimental setup. (**A**) Pairs of photons are generated via spontaneous parametric down-conversion in a periodically poled KTP crystal, using the Sagnac design of Fedrizzi *et al.* (*48*). The degree of polarization entanglement between the two photons can be continuously varied by changing the polarization angle γ of the pump laser. Alice and Bob perform measurements in the equatorial plane of the Bloch sphere using a half-wave plate (HWP) and a polarizing beam splitter (PBS). Additional quarter-wave plates (QWPs) can be used for quantum state tomography of the initial entangled state. In the interventionist experiment, an additional combination of QWP and polarizer (POL) is used between Alice's basis choice and her measurement. Causal variables are indicated using the notation of Fig. 1A. Note that Λ can represent an arbitrary hidden variable acting as a common cause for the observed outcomes, which need not necessarily originate at the source. (**B**) Alice's (red) and Bob's (blue) measurement bases and the intervention direction (cyan) on the Bloch sphere. QRNG, quantum random number generator; APD, avalanche photodiode.

$\mathrm{ACE}_{A\rightarrow B}$, were computed from a total of 48,000 coincidence counts, and no more than one event was registered for each set of random choices for X, Y, and the two elements of I.

Figure 3 shows the observed average causal effect as a function of the CHSH values measured for a range of entangled states. All measured values are below $\mathrm{ACE}_{A\rightarrow B} = 0.02^{+0.02}_{-0.02}$ and largely independent of the observed CHSH violation. Note that the quantity is bounded from below, which results in non-Gaussian statistics and makes the value 0 unachievable in the presence of experimental imperfections and finite counting statistics. When taking this into account, all data lie within the 3σ noise due to Poissonian counting statistics (see the Supplementary Materials for details). All quoted uncertainties were obtained from Monte Carlo simulations of the Poissonian counting statistics and correspond to the 0.13th and 99.87th percentile, respectively (in the case of normally distributed variables, this would correspond to 3σ confidence regions). Within current experimental capabilities, we find that CHSH violations above a value of $S_2 = 2.05 \pm 0.02$ cannot be fully explained by means of a direct causal influence from one outcome to the other. That is, the potential causal influence between Alice's and Bob's measurement (green arrow in Fig. 1B) is not sufficiently strong.

Observational method

As we have demonstrated, interventions can be used to distinguish direct causation from common-cause correlations in the two-setting CHSH test, which is not possible with passive observation alone. However, this comes at the cost that the intervention relies on the quantum description of the degree of freedom responsible for the outcome A (in the case above, the polarization). The interventional method is thus necessarily device-dependent and cannot be used to test arbitrary hidden-variable models. We now show how moving beyond the CHSH scenario allows for a device-independent test of any model with an arbitrarily strong causal influence from one outcome to the other.

Consider the situation where each of the two parties can choose to measure one of three different dichotomic observables. As shown in

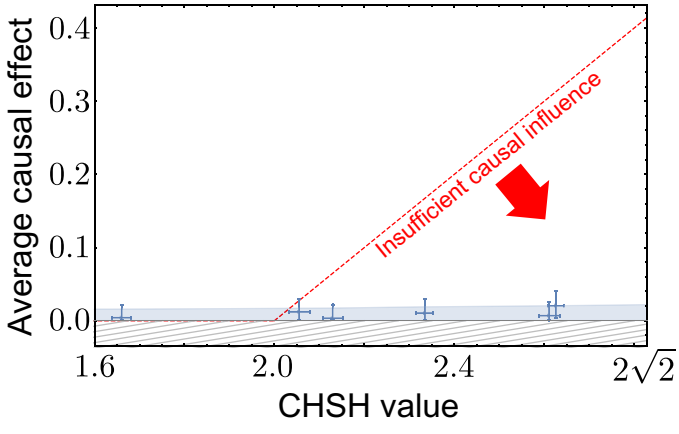

Fig. 3. Observed average causal effect ACE versus measured CHSH value. Any value below the dashed red line, given by Eq. 4, is not sufficient to explain the observed CHSH violation. Note that the quantity ACE is bounded from below by 0, as indicated by the hatched area, resulting in asymmetric error distributions. The blue shaded area represents the 3σ region of Poissonian noise. All errors represent the 3σ statistical confidence intervals obtained from a Monte Carlo simulation of the Poissonian counting statistics.

the work of Chaves *et al.* (*11*), any correlations compatible with the model in Fig. 1B must now satisfy

$$S_3 = \langle E_{00}\rangle - \langle E_{02}\rangle - \langle E_{11}\rangle + \langle E_{12}\rangle - \langle E_{20}\rangle + \langle E_{21}\rangle \leq 4 \quad (5)$$

This inequality is symmetric under exchange of the parties and, as we show in the Supplementary Materials, satisfied by any model that contains communication of outcomes from Alice to Bob, Bob to Alice, or any mixture thereof. Crucially, this allows us to test the models in Fig. 1B in a device-independent fashion and without committing to any particular temporal ordering of *A* and *B*.

To test inequality (*5*), Alice and Bob each perform measurements on their quantum system along one of three directions in the equatorial plane of the Bloch sphere. These measurements are implemented using the setup in Fig. 2, with the intervention elements *I* removed. The specific measurement settings are given in the Supplementary Materials. Figure 4 shows the observed violation of inequality (*5*) as a function of the parameter γ of the used quantum state. The theoretical maximal violation of the inequality is achieved using a maximally entangled state, corresponding to γ = 45°.

We observe a value of up to $S_3 = 5.16^{+0.02}_{-0.02}$, corresponding to a violation of Eq. 5 by more than 170 SDs. Complementary to the interventional experiment, which rules out outcome-dependent causal models in the CHSH scenario but requires additional assumptions about the underlying causal mechanisms, this result rules out outcome-dependent causal models without additional assumptions in any scenario with more than two settings. A direct causal influence from one outcome to the other can therefore not explain quantum correlations.

DISCUSSION

Previous work on causal explanations beyond local hidden-variable models focused on testing Leggett's crypto-nonlocality (*7*, *42*, *43*), a class of models with a very specific choice of hidden variable that is unrelated to Bell's local causality (*44*). In contrast, we make no assumptions on the form of the hidden variable and test all models compatible with the causal structure in Fig. 1B, which is a natural generalization of Bell-local models and contains them as a special case. Practically, our experiment relies on a fair-sampling assumption (see the Supplementary Materials). Causal models are formulated without any reference to space-time structure, and hence, space-like separation between *A* and *B* is not required. Our results demonstrate that a causal influence from one measurement outcome to the other, which may be subluminal, superluminal, or even instantaneous, cannot explain the observed correlations.

Our results could have applications in quantum cryptography scenarios where the secrecy of the measurement outcomes cannot be

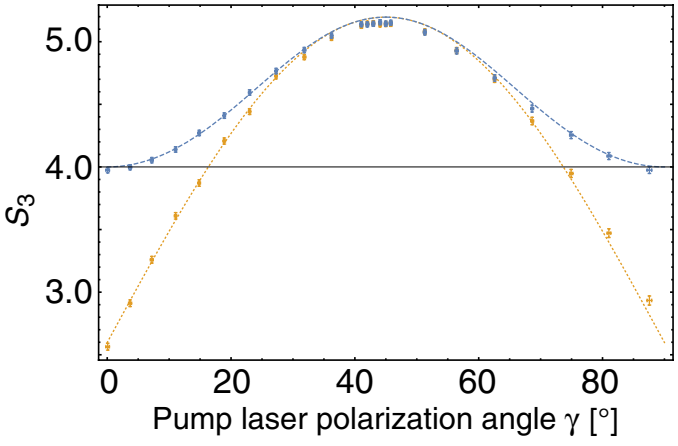

Fig. 4. Observed values S_3 for a variety of quantum states of the form cosγ|*HV*⟩ + sinγ|*VH*⟩. The orange data points are observed using a fixed measurement scheme (optimal for the maximally entangled state γ = 45°), with the dotted, orange line representing the corresponding theory prediction. The blue data points and blue dashed theory line correspond to the case where measurement settings were optimized for the prepared states (see the Supplementary Materials for details). The black line represents the bound of inequality (*5*); any point above this line cannot be explained causally by a model of the form in Fig. 1B. Error bars correspond to 3σ statistical confidence intervals.

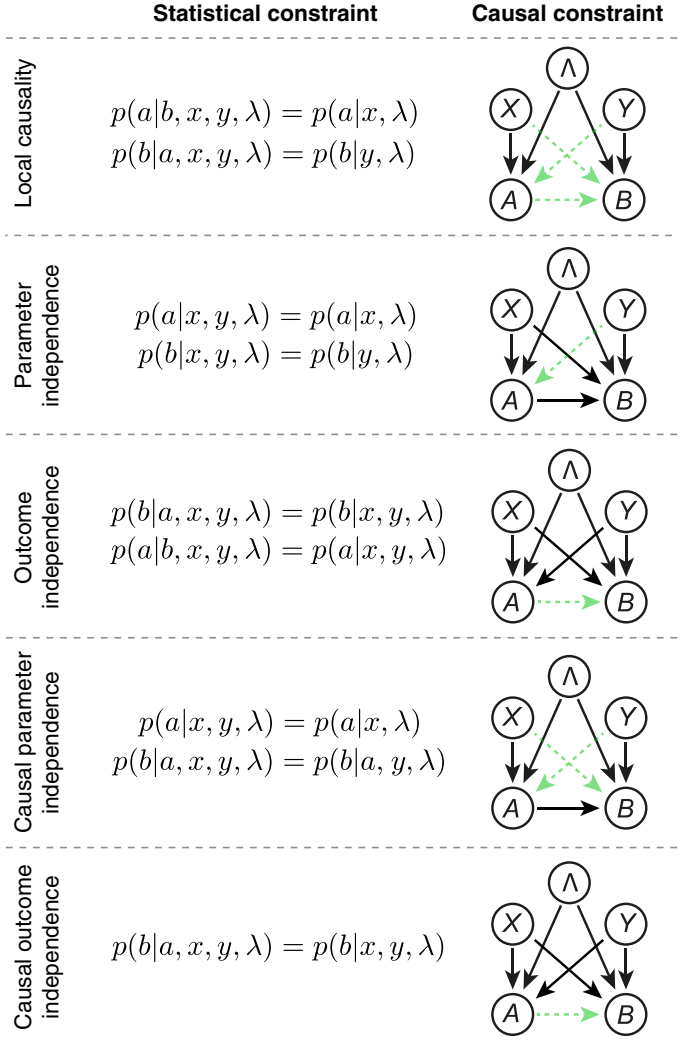

Fig. 5. Comparison of various constraints on the causal structure of Bell's theorem. The causal links forbidden by the respective assumption are shown in dashed green lines. Note that the statistical constraints implied by causal parameter independence are asymmetric in *a* and *b*, and swapping them would result in a causal structure where the arrow between *A* and *B* is reversed. Our experimental test applies to both of these structures and any convex combination of them.

guaranteed. Consider a one-sided device-independent scenario where Alice's laboratory is trusted, but an eavesdropper, Eve, may control Bob's devices and the source of particles. In a standard quantum key distribution protocol, Alice and Bob would first attempt to violate the CHSH inequality to certify that they share entanglement. However, using the knowledge of Alice's measurement outcomes, Eve could convincingly produce outcomes for Bob that simulate such a violation. Using an intervention on her measurement outcome, Alice can reveal such an attack as a nonzero value of $ACE_{A\to B}$ (see Eq. 4). Alternatively, Alice and Bob could use inequality (*5*) to certify that they share entanglement because a violation of this inequality cannot be simulated by Eve using knowledge of Alice's measurement outcomes.

It will be of considerable interest to further develop the causal modeling tools demonstrated here to test other classes of causal models, for example, allowing for retrocausal influences or relaxations of measurement independence (*8*–*14*, *45*). Alternatively, one could completely abandon the classical notion of causality and pursue a novel framework of quantum causality (*21*, *24*–*27*). It was recently shown that such a framework can be based on interventionist causation, which allows for causal discovery and recovers the classical causal modeling framework in the appropriate limit (*46*).

Recent experiments put strong constraints on realist interpretations of quantum mechanics, ruling out maximally epistemic (*47*) and local causal (*3*–*5*) models. Our results exclude a broad class of nonlocal causal models, thus contributing to a clearer picture of the status of reality and causality in quantum mechanics.

MATERIALS AND METHODS

Causal interpretation of local causality

Local causality captures the idea that there should be no causal influence from one side of the experiment to the spacelike separated other side. Formally, this is a constraint on the conditional probability distributions: $p(a|b,x,y,\lambda) = p(a|x,\lambda)$ and $p(b|a,x,y,\lambda) = p(b|y,\lambda)$. We would like to stress that local causality is not equivalent to signal locality, which follows from special relativity and imposes constraints on the observable probabilities only: $p(a|x, y) = p(a|x)$ and $p(b|x, y) = p(b|y)$. The natural generalization of signal locality to include the hidden variable is typically referred to as parameter independence or locality: $p(a|x,y,\lambda) = p(a|x,\lambda)$ and $p(b|x,y,\lambda) = p(b|y,\lambda)$ (*36*). Parameter independence, together with what is often referred to as outcome independence $p(a|b,x,y,\lambda) = p(a|x,y,\lambda)$ and $p(b|a,x,y,\lambda) = p(b|x,y,\lambda)$, then implies local causality.

Interpreted in the causal modeling framework, local causality implies that there is no causal link from Bob's measurement setting Y or outcome B to Alice's measurement outcome A, and similarly from Alice to Bob (compare Fig. 5). In the spirit of causal modeling, we would like to obtain the causal structure of Bell's theorem directly from investigating these causal independencies. Specifically, causal outcome independence denotes the absence of a causal link between the measurement outcomes, and causal parameter independence denotes the absence of a causal link from each party's setting to the other's outcome. The latter condition still allows causal influence between measurement outcomes. Because no causal loop can exist, in a single causal model, this link must be either from A to B or from B to A. The most general correlations consistent with causal parameter independence are convex combinations of correlations consistent with either model.

As shown in Fig. 5, the causal models compatible with causal outcome independence are the same as for ordinary outcome independence. Causal parameter independence, on the other hand, imposes different constraints than "ordinary" parameter independence. The latter is defined as the conjunction of the statistical constraints for Alice and Bob. Either of these can be given a causal interpretation in terms of a causal model, which, when imposing the constraint for Alice, contains explicit links from X and A to B (compare Fig. 5), and similarly for Bob. However, the set of probability distributions that satisfy both constraints does not correspond to a causal model, unless outcome independence is assumed as well. In contrast, causal parameter independence is defined such that there are no causal links from X to B and Y to A, but a link between A and B (compare Fig. 5 for the case $A\to B$) is allowed. Because there are two possible directions for this link, causal parameter independence contains a set of constraints for each model, and the set of probability distributions compatible with it is the set of those compatible with either model.

Note that the joint assumption of causal parameter independence and causal outcome independence is equivalent to local causality and thus equivalent to the joint assumption of ordinary parameter independence and ordinary outcome independence. However, in contrast to the latter pair, our causal assumptions individually have clear causal interpretations.

SUPPLEMENTARY MATERIALS

Supplementary material for this article is available at http://advances.sciencemag.org/cgi/content/full/2/8/e1600162/DC1

Relaxation of local causality

Theoretical analysis of experimental imperfections

Testing the new inequality

Error analysis

fig. S1. Efficiency η and visibility *v* requirements for a violation of inequality (*5*) in the main text without fair-sampling assumption.

fig. S2. Measurement angles for inequality (*5*) in the main text.

fig. S3. Distribution of statistical noise due to Poissonian counting statistics.

table S1. Wave plate characterization data.

References (*49*–*54*)

REFERENCES AND NOTES

1. S. J. Freedman, J. F. Clauser, Experimental test of local hidden-variable theories. *Phys. Rev. Lett.* **28**, 938–941 (1972).
2. J. S. Bell, On the Einstein–Podolsky–Rosen paradox. *Physics* **1**, 195–290 (1964).
3. B. Hensen, H. Bernien, A. E. Dréau, A. Reiserer, N. Kalb, M. S. Blok, J. Ruitenberg, R. F. L. Vermeulen, R. N. Schouten, C. Abellán, W. Amaya, V. Pruneri, M. W. Mitchell, M. Markham, D. J. Twitchen, D. Elkouss, S. Wehner, T. H. Taminiau, R. Hanson, Loophole-free Bell inequality violation using electron spins separated by 1.3 kilometres. *Nature* **526**, 682–686 (2015).
4. L. K. Shalm, E. Meyer-Scott, B. G. Christensen, P. Bierhorst, M. A. Wayne, M. J. Stevens, T. Gerrits, S. Glancy, D. R. Hamel, M. S. Allman, K. J. Coakley, S. D. Dyer, C. Hodge, A. E. Lita, V. B. Verma, C. Lambrocco, E. Tortorici, A. L. Migdall, Y. Zhang, D. R. Kumor, W. H. Farr, F. Marsili, M. D. Shaw, J. A. Stern, C. Abellán, W. Amaya, V. Pruneri, T. Jennewein, M. W. Mitchell, P. G. Kwiat, J. C. Bienfang, R. P. Mirin, E. Knill, S. W. Nam, Strong loophole-free test of local realism. *Phys. Rev. Lett.* **115**, 250402 (2015).
5. M. Giustina, M. A. M. Versteegh, S. Wengerowsky, J. Handsteiner, A. Hochrainer, K. Phelan, F. Steinlechner, J. Kofler, J.-Å. Larsson, C. Abellán, W. Amaya, V. Pruneri, M. W. Mitchell, J. Beyer, T. Gerrits, A. E. Lita, L. K. Shalm, S. W. Nam, T. Scheidl, R. Ursin, B. Wittmann, A. Zeilinger, Significant-loophole-free test of Bell's theorem with entangled photons. *Phys. Rev. Lett.* **115**, 250401 (2015).
6. C. H. Brans, Bell's theorem does not eliminate fully causal hidden variables. *Int. J. Theor. Phys.* **27**, 219–226 (1988).

7. C. Branciard, N. Brunner, N. Gisin, C. Kurtsiefer, A. Lamas-Linares, A. Ling, V. Scarani, Testing quantum correlations versus single-particle properties within Leggett's model and beyond. *Nat. Phys.* **4**, 681–685 (2008).
8. M. J. W. Hall, Local deterministic model of singlet state correlations based on relaxing measurement independence. *Phys. Rev. Lett.* **105**, 250404 (2010).
9. M. J. W. Hall, Relaxed Bell inequalities and Kochen-Specker theorems. *Phys. Rev. A* **84**, 022102 (2011).
10. J. Barrett, N. Gisin, How much measurement independence is needed to demonstrate nonlocality? *Phys. Rev. Lett.* **106**, 100406 (2011).
11. R. Chaves, R. Kueng, J. B. Brask, D. Gross, Unifying framework for relaxations of the causal assumptions in Bell's theorem. *Phys. Rev. Lett.* **114**, 140403 (2015).
12. C. J. Wood, R. W. Spekkens, The lesson of causal discovery algorithms for quantum correlations: Causal explanations of Bell-inequality violations require fine-tuning. *New J. Phys.* **17**, 033002 (2015).
13. D. Aktas, S. Tanzilli, A. Martin, G. Pütz, R. Thew, N. Gisin, Demonstration of quantum nonlocality in the presence of measurement dependence. *Phys. Rev. Lett.* **114**, 220404 (2015).
14. G. Pütz, N. Gisin, Measurement dependent locality. *New J. Phys.* **18**, 055006 (2016).
15. J. Pearl, *Causality* (Cambridge Univ. Press, Cambridge, 2009).
16. P. Spirtes, N. Glymour, R. Scheines, *Causation, Prediction, and Search* (MIT Press, Cambridge, ed. 2, 2001), 568 pp.
17. D. Geiger, C. Meek, Quantifier elimination for statistical problems, Proceedings of the 15th Conference on Uncertainty in Artificial Intelligence, Stockholm, Sweden, 30 to 31 July 1999, pp. 226–235.
18. J. Tian, J. Pearl, On the testable implications of causal models with hidden variables, *Proceedings of the Eighteenth Conference on Uncertainty in Artificial Intelligence*, Alberta, Canada, 1 to 4 August 2002, pp. 519–527.
19. R. Chaves, L. Luft, T. O. Maciel, D. Gross, D. Janzing, B. Schölkopf, Inferring latent structures via information inequalities, *Proceedings of the 30th Conference on Uncertainty in Artificial Intelligence*, Quebec, Canada, 23 to 27 July 2014, pp. 112–121.
20. J. M. Mooij, J. Peters, D. Janzing, J. Zscheischler, B. Schölkopf, Distinguishing cause from effect using observational data: Methods and benchmarks. *J. Mach. Learn. Res.* **17**, 1–102 (2016).
21. R. Chaves, C. Majenz, D. Gross, Information–theoretic implications of quantum causal structures. *Nat. Commun.* **6**, 5766 (2015).
22. T. Fritz, Beyond Bell's theorem: Correlation scenarios. *New J. Phys.* **14**, 103001 (2012).
23. T. Fritz, Beyond Bell's theorem II: Scenarios with arbitrary causal structure. *Commun. Math. Phys.* **341**, 391–434 (2016).
24. E. G. Cavalcanti, R. Lal, On modifications of Reichenbach's principle of common cause in light of Bell's theorem. *J. Phys. A Math. Theor.* **47**, 424018 (2014).
25. J. Pienaar, Č. Brukner, A graph-separation theorem for quantum causal models. *New J. Phys.* **17**, 073020 (2015).
26. M. S. Leifer, R. W. Spekkens, Towards a formulation of quantum theory as a causally neutral theory of Bayesian inference. *Phys. Rev. A* **88**, 052130 (2013).
27. J. Henson, R. Lal, M. F. Pusey, Theory-independent limits on correlations from generalized Bayesian networks. *New J. Phys.* **16**, 113043 (2014).
28. P. M. Näger, The causal problem of entanglement. *Synthese* **193**, 1127–1155 (2016).
29. O. Oreshkov, C. Giarmatzi, Causal and causally separable processes. arXiv:1506.05449 (2015).
30. Č. Brukner, Quantum causality. *Nat. Phys.* **10**, 259–263 (2014).
31. G. Chiribella, G. M. D'Ariano, P. Perinotti, B. Valiron, Quantum computations without definite causal structure. *Phys. Rev. A* **88**, 022318 (2013).
32. G. Chiribella, Perfect discrimination of no-signalling channels via quantum superposition of causal structures. *Phys. Rev. A* **86**, 040301(R) (2012).
33. M. Araújo, F. Costa, Č. Brukner, Computational advantage from quantum-controlled ordering of gates. *Phys. Rev. Lett.* **113**, 250402 (2014).
34. L. M. Procopio, A. Moqanaki, M. Araújo, F. Costa, I. Alonso Calafell, E. G. Dowd, D. R. Hamel, L. A. Rozema, Č. Brukner, P. Walther, Experimental superposition of orders of quantum gates. *Nat. Commun.* **6**, 7913 (2015).
35. J. F. Clauser, M. A. Horne, A. Shimony, R. A. Holt, Proposed experiment to test local hidden-variable theories. *Phys. Rev. Lett.* **23**, 880–884 (1969).
36. H. M. Wiseman, E. G. Cavalcanti, *Causarum Investigatio* and the two Bell's theorems of John Bell. arXiv:1503.06413 (2015).
37. J.-D. Bancal, S. Pironio, A. Acín, Y.-C. Liang, V. Scarani, N. Gisin, Quantum non-locality based on finite-speed causal influences leads to superluminal signalling. *Nat. Phys.* **8**, 867–870 (2012).
38. D. Janzing, D. Balduzzi, M. Grosse-Wentrup, B. Schölkopf, Quantifying causal influences. *Ann. Stat.* **41**, 2324–2358 (2013).
39. K. Ried, M. Agnew, L. Vermeyden, D. Janzing, R. W. Spekkens, K. J. Resch, A quantum advantage for inferring causal structure. *Nat. Phys.* **11**, 414–420 (2015).
40. S. Hill, W. K. Wootters, Entanglement of a pair of quantum bits. *Phys. Rev. Lett.* **78**, 5022–5025 (1997).
41. T. Symul, S. M. Assad, P. K. Lam, Real time demonstration of high bit rate quantum random number generation with coherent laser light. *Appl. Phys. Lett.* **98**, 231103 (2011).
42. S. Gröblacher, T. Paterek, R. Kaltenbaek, Č. Brukner, M. Żukowski, M. Aspelmeyer, A. Zeilinger, An experimental test of non-local realism. *Nature* **446**, 871–875 (2007).
43. T. Paterek, A. Fedrizzi, S. Gröblacher, T. Jennewein, M. Żukowski, M. Aspelmeyer, A. Zeilinger, Experimental test of nonlocal realistic theories without the rotational symmetry assumption. *Phys. Rev. Lett.* **99**, 210406 (2007).
44. C. Branciard, Bell's local causality, Leggett's crypto-nonlocality, and quantum separability are genuinely different concepts. *Phys. Rev. A* **88**, 042113 (2013).
45. J. Gallicchio, A. S. Friedman, D. I. Kaiser, Testing Bell's inequality with cosmic photons: Closing the setting-independence loophole. *Phys. Rev. Lett.* **112**, 110405 (2014).
46. F. Costa, S. Shrapnel, Quantum causal modelling. *New J. Phys.* **18**, 063032 (2016).
47. M. Ringbauer, B. Duffus, C. Branciard, E. G. Cavalcanti, A. G. White, A. Fedrizzi, Measurements on the reality of the wave function. *Nat. Phys.* **11**, 249–254 (2015).
48. A. Fedrizzi, T. Herbst, A. Poppe, T. Jennewein, A. Zeilinger, A wavelength-tunable fiber-coupled source of narrowband entangled photons. *Opt. Express* **15**, 15377–15386 (2007).
49. S. Popescu, D. Rohrlich, Quantum nonlocality as an axiom. *Found. Phys.* **24**, 379–385 (1994).
50. C. Uhler, G. Raskutti, P. Bühlmann, B. Yu, Geometry of the faithfulness assumption in causal inference. *Ann. Stat.* **41**, 436–463 (2013).
51. T. Christof, A. Löbel, PORTA—POlyhedron Representation Transformation Algorithm (2009); http://comopt.ifi.uni-heidelberg.de/software/PORTA/.
52. P. H. Eberhard, Background level and counter efficiencies required for a loophole-free Einstein-Podolsky-Rosen experiment. *Phys. Rev. A* **47**, R747–R750 (1993).
53. J. Wilms, Y. Disser, G. Alber, I. C. Percival, Local realism, detection efficiencies, and probability polytopes. *Phys. Rev. A* **78**, 032116 (2008).
54. R. Chaves, J. B. Brask, Feasibility of loophole-free nonlocality tests with a single photon. *Phys. Rev. A* **84**, 062110 (2011).

Acknowledgments: We thank C. Branciard, E. Cavalcanti, and H. Wiseman for helpful discussions. We also thank the team from the Austrian Institute of Technology for providing the time-tagging modules for this experiment. **Funding:** This work was supported, in part, by the Centre for Engineered Quantum Systems (CE110001013), the Centre for Quantum Computation and Communication Technology (CE110001027), and the Templeton World Charity Foundation (TWCF 0064/AB38). R.C. acknowledges support from the Excellence Initiative of the German Federal and State Governments (grants ZUK 43 and ZUK 81), the U.S. Army Research Office under contracts W911NF-14-1-0098 and W911NF- 14-1-0133 (Quantum Characterization, Verification, and Validation), the DFG (GRO 4334 and SPP 1798), and the Brazilian ministries MEC and MCTIC. A.G.W. acknowledges support through a University of Queensland Vice-Chancellor's Senior Research and Teaching Fellowship and A.F. through an Australian Research Council Discovery Early Career Award (DE130100240). **Author contributions:** M.R., R.C., and A.F. conceived the study. A.F., A.G.W., M.R., C.G., and F.C. designed the experiment. R.C. derived the theory results. M.R. and C.G. performed the experiment and collected and analyzed data. All authors contributed to writing the manuscript. **Competing interests:** The authors declare that they have no competing interests. **Data and materials availability:** All data needed to evaluate the conclusions in the paper are present in the paper and/or the Supplementary Materials. Additional data related to this paper may be requested from the authors.

Submitted 28 January 2016
Accepted 11 July 2016
Published 10 August 2016
10.1126/sciadv.1600162

Citation: M. Ringbauer, C. Giarmatzi, R. Chaves, F. Costa, A. G. White, A. Fedrizzi, Experimental test of nonlocal causality. *Sci. Adv.* **2**, e1600162 (2016).

ScienceAdvances
AAAS

Experimental test of nonlocal causality

Martin Ringbauer, Christina Giarmatzi, Rafael Chaves, Fabio Costa, Andrew G. White and Alessandro Fedrizzi (August 10, 2016)

Sci Adv 2016, 2:.
doi: 10.1126/sciadv.1600162